Fusion of ^{46}Ti+^{46}Ti near the Coulomb barrier

A. M. Stefanini, M. Trotta, L. Corradi, and A. M. Vinodkumar
Istituto Nazionale di Fisica Nucleare, Laboratori Nazionali di Legnaro, I-35020 Legnaro, Padova, Italy

F. Scarlassara, G. Montagnoli, and S. Beghini
Dipartimento di Fisica, Universitá di Padova, and Istituto Nazionale di Fisica Nucleare, Sezione di Padova, I-35131 Padova, Italy

(Received 12 November 2001; published 15 February 2002)

Fusion cross sections have been measured for the symmetric system ^{46}Ti+^{46}Ti in the energy range encompassing the Coulomb barrier. A representation of the fusion barrier distribution has been obtained from the second energy derivative of the excitation function. The data are well described by coupled-channels calculations including two quadrupole phonons and one octupole phonon of both colliding nuclei. The comparison with previous data for ^{40}Ca+^{46}Ti and ^{40}Ca+^{40}Ca clarifies the relative importance of various low-lying inelastic exitations of ^{46}Ti and of ^{40}Ca in the subbarrier fusion yields. Similarities with the case of ^{58}Ni+^{60}Ni are pointed out.

DOI: 10.1103/PhysRevC.65.034609 PACS number(s): 25.70.Jj, 27.40.+z

I. INTRODUCTION

Heavy-ion fusion near and below the Coulomb barrier is strongly influenced by the nuclear structure of the colliding ions (see, e.g., Refs. [1,2]). The study of fusion barrier distributions, extracted as the second energy derivative of fusion excitation functions [3], has been a breakthrough in enlightening the role played by couplings to collective degrees of freedom. Early experiments [4,5] concerned reactions where heavy deformed targets (^{154}Sm, ^{186}W) were bombarded by ^{16}O; subsequently, the use of a ^{40}Ca beam allowed us to observe [6] the different effects caused by the prolate and oblate deformation of ^{192}Os and ^{194}Pt. Very recently, the influence of higher-order deformations in the fusion of ^{168}Er with ^{34}S has been shown [7]. In parallel, detailed investigations of systems such as ^{16,17}O+^{144}Sm [8], ^{58}Ni+^{60}Ni [9], and ^{40}Ca+^{90,96}Zr [10] were carried out, where the prominent influence of low-lying inelastic excitations was clearly shown, along with the possible role played by neutron transfer channels. Recently, the detailed study of ^{36}S+^{90,96}Zr [11] has allowed us to single out the effect introduced by the strong octupole vibration in ^{96}Zr.

In particular, the characteristic structures produced in the barrier distribution by multiphonon excitations was first shown by the study of the ''quasisymmetric'' system ^{58}Ni +^{60}Ni [9]. Hence the investigation of fusion between identical nuclei with well-known collective excitations at low energies is interesting in order to further clarify the influence of such inelastic states on fusion. The symmetry of the system allows one to deduce the effect of the quadrupole (or octupole) phonon that is present in the projectile as well as in the target nucleus, in a favorable condition. We chose the case of ^{46}Ti+^{46}Ti, since this nuclide has a low-energy structure with collective excitations among the strongest ones known in the mass region $A \approx 40$–60, and the 2^+ state lies at 889 keV only. The octupole vibration is weak and above 3 MeV, hence its effect on fusion should be less important.

Further interest in the study of ^{46}Ti+^{46}Ti arises from the possibility of a comparative analysis with the two systems ^{40}Ca+^{40}Ca and ^{40}Ca+^{46}Ti. The fusion excitation function of ^{40}Ca+^{40}Ca was measured a long time ago [12], and provides a reference case with a barrier distribution showing a single peak characteristic of the collision between two spherical rigid nuclei. The intermediate case ^{40}Ca+^{46}Ti is also known [13] and its barrier distribution has two peaks. This will help to clarify the transition from the spherical case to the strongly collective ^{46}Ti+^{46}Ti system.

Transfer couplings are not expected to be important in any of the three combinations involving ^{46}Ti and ^{40}Ca, since neutron and proton transfer Q values are largely negative in all cases.

Section II of this paper presents the experimental setup and the measurements, together with the experimental data; in Sec. III a full comparison is done with the previous data for ^{40}Ca+^{40}Ca and ^{40}Ca+^{46}Ti; Sec. IV reports about the data analysis within the coupled-channels model, and the analogies with the case of ^{58}Ni+^{60}Ni are pointed out. The most relevant conclusions are summarized in Sec. V.

II. EXPERIMENT

The experiment has been performed using the ^{46}Ti beam of the XTU Tandem accelerator of the Laboratori Nazionali di Legnaro of Istituto Nazionale di Física Nucleare. A TiH sample enriched to around 77% in mass 46 was introduced in the sputter ion source. The accelerated beams had typical intensities 5–10 pnA and energies in the range 116.0 to 142.0 MeV, and the targets were evaporations of ^{46}Ti (50 μg/cm^2) on carbon backings (15 μg/cm^2) facing the beam. The target isotopic enrichment was 96.84%; the presence of small amounts of heavier titanium isotopes introduced small corrections to the measured evaporation residue yields. The beam energy loss across the carbon backing and half of the ^{46}Ti target was $\simeq$900 keV, depending on the energy, and it was taken into account in the data reduction.

The fusion-evaporation residues (ER) were detected at 0° and at small angles by using an electrostatic deflector [14] that separated out the beam and beamlike particles. The ER were then identified by a time-of-flight energy (E) telescope consisting of a microchannel plate detector and (40 cm

TABLE I. Fusion cross sections of ^{46}Ti+^{46}Ti measured in this work. Energies are in the center of mass system; quoted errors are pure statistical uncertainties.

E (MeV)	σ_{ER} (mb)	E (MeV)	σ_{ER} (mb)
58.0	0.45±0.15	65.0	113.5±2.1
58.5	0.56±0.14	65.5	141.4±2.4
59.0	1.77±0.27	66.0	159.5±2.3
59.5	3.24±0.27	66.5	171.8±3.5
60.0	5.33±0.45	67.0	216.0±4.4
60.5	9.06±0.49	67.5	227.9±3.0
61.0	12.74±0.52	68.0	273.6±3.2
61.5	21.22±0.65	68.5	297.0±3.3
62.0	29.25±1.06	69.0	329.0±3.6
62.5	39.9±1.2	69.5	338.6±3.8
63.0	43.6±2.1	70.0	342.6±4.3
63.5	62.7±1.6	70.5	383.5±4.4
64.0	80.7±2.1	71.0	372.4±5.7
64.5	93.3±2.1		

downstream) of a 300 mm^2 silicon surface-barrier detector. The transmission of the electrostatic deflector was estimated to be 0.67±0.07 by Monte Carlo calculations (see Refs. [11,15]). Four monitor detectors were placed at $\theta \simeq 16°$, symmetrically around the beam direction. More details of the setup and of the experimental procedure can be found in the recent paper [11] reporting on the study of ^{36}S+^{90,96}Zr.

The zero degree excitation function was measured in a single sequence of runs with energy step $\Delta E_{lab}=1.0$ MeV, starting from the highest energy 142 MeV. The ER angular distribution was measured at $E_{lab}=130$ MeV in the range $-6°$ to $+4°$ with steps of one degree. The energy dependence of the width and shape of the angular distribution is expected to be very small in the energy range of the excitation function, as actually observed in our previous experiments on near-barrier fusion (see Refs. [10,11]). The measured angular distribution for ^{46}Ti+^{46}Ti is symmetrical around the nominal 0° and drops by a factor ≈30 at 6°.

Since fusion-fission is negligible, total fusion cross sections were obtained by integrating the angular distribution at 130 MeV and by the 0° yields normalized to the elastic counts into the monitors, and the (small) correction for Mott scattering was included. The accuracy of the absolute cross section scale is estimated to be ±14% (see Refs. [9,11] for more details), where the errors on the transmission of the deflector, on the angular distribution measurement, and on the detectors solid angles are taken into account. Statistical uncertainties (determining relative errors) are much smaller, i.e., around 1% above or around the barrier, increasing up to ≈20% at the lowest energies.

Table I reports the cross sections measured in this work and Fig. 1 is the corresponding plot. The fusion barrier distribution of ^{46}Ti+^{46}Ti was extracted as the second energy derivative of the excitation function [3], approximated by the three-point difference formula [10] with a step $\Delta E_{lab}=2$ MeV (using $\Delta E_{lab}=1$ MeV leads to very large error bars). The barrier distribution is shown in Fig. 2 where the ordinate B is normalized to πR_b^2, and R_b is the barrier radius obtained from the Akyüz-Winther potential [16]. We observe two peaks, ≈2.2–2.4 MeV wide (full width at half maximum), at approximately 61 MeV and 64 MeV; points above 68 MeV are not reported because of the very large uncertainties.

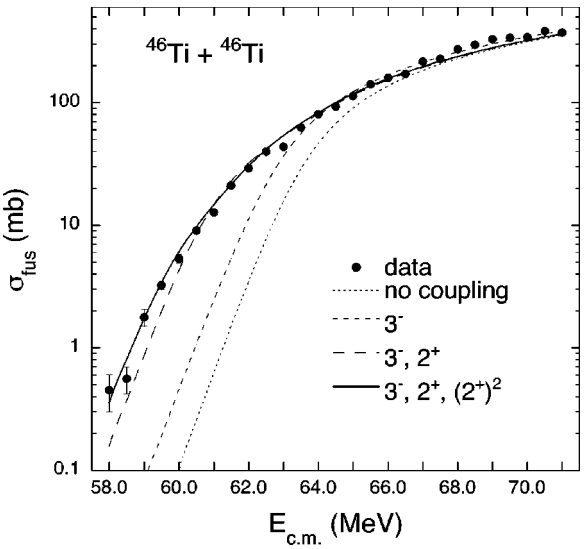

FIG. 1. The excitation function of ^{46}Ti+^{46}Ti, as measured in this work (dots), is compared with the results of coupled-channels calculations; see text for more details.

III. COMPARING WITH NEARBY SYSTEMS

The fusion cross sections of ^{46}Ti+^{46}Ti measured in this work are plotted in Fig. 3 together with the previous data for ^{40}Ca+^{40}Ca [12] and for the intermediate system ^{40}Ca +^{46}Ti [13], in a reduced energy scale that takes into account the different Coulomb barriers calculated from the Akyüz-Winther potential [16]. We point out that the excitation func-

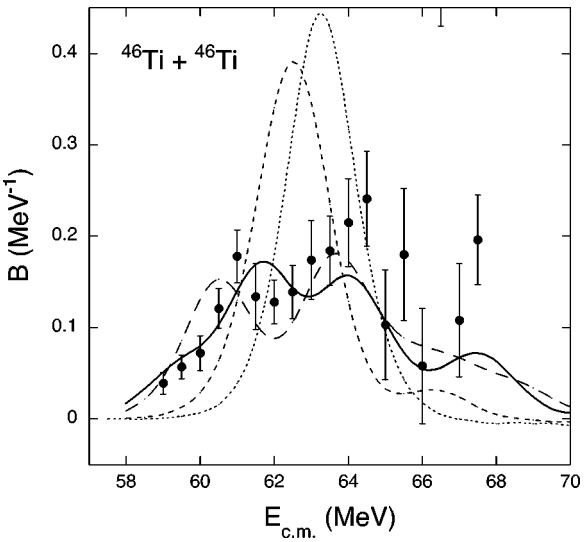

FIG. 2. The fusion barrier distribution extracted from the excitation function of ^{46}Ti+^{46}Ti (dots), and the distributions calculated by the CC model; the legend is the same as for Fig. 1.

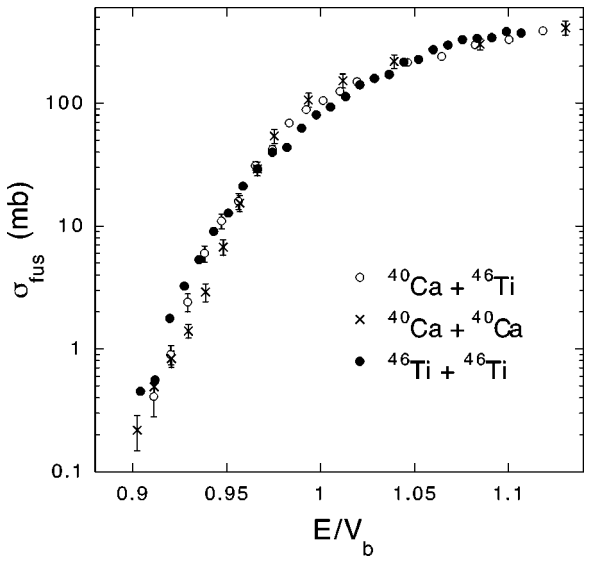

FIG. 3. Fusion cross sections of ^{46}Ti+^{46}Ti (dots), ^{40}Ca+^{46}Ti (open dots) [13], and ^{40}Ca+^{40}Ca (crosses) [12] in a reduced energy scale. The excitation functions of the three systems are similar to each other in this representation.

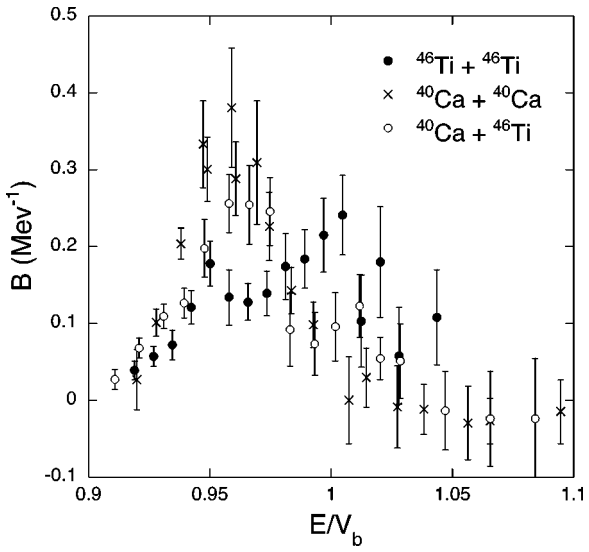

FIG. 4. Barrier distributions of ^{46}Ti+^{46}Ti (dots), ^{40}Ca+^{46}Ti (open dots) [13], and ^{40}Ca+^{40}Ca (crosses, taken from Ref. [2]) in a reduced energy scale. The three barrier distributions are very different from each other.

tions of ^{40}Ca+^{40}Ca and that of ^{40}Ca+^{46}Ti were successfully reproduced [17,13] by coupled-channels calculations including low-lying inelastic excitations and transfer couplings as well, although much less important.

At a first glance (Fig. 3), the three excitation functions do not look very different from each other in the whole energy range, apart from a small relative enhancement visible for ^{46}Ti+^{46}Ti at subbarrier energies, at variance with the naive expectation that the strong low-lying (E_x=0.889 MeV) 2^+ state of ^{46}Ti would imply much larger fusion cross sections below the barrier for systems involving that nucleus, with respect to the fusion of two magic ^{40}Ca nuclei. Actually, although having a rigid, double closed-shell structure, ^{40}Ca shows a very strong octupole vibration at 3.737 MeV that greatly increases the subbarrier fusion yields compared to the one-dimensional penetration of the Coulomb barrier, since the main consequence of that high-energy excitation is renormalizing the bare ion-ion potential. Similar fusion cross sections are observed in the reduced energy scale of Fig. 3 for ^{40}Ca+^{46}Ti, where one has the concurring effect of the octupole and quadrupole excitations of the two colliding nuclei. Replacing, further, ^{40}Ca with a second ^{46}Ti does not bring large additional effects, at the level of comparing the near-barrier and subbarrier excitation functions.

Actually, differences between the three excitation functions are present. The data for ^{40}Ca+^{40}Ca fall down more steeply with energy between 100 mb and 1 mb, while the cross sections for ^{46}Ti+^{46}Ti are lower than for the other two cases at energies around the Coulomb barrier. By using the ''enlarging lens'' offered by the technique of extracting barrier distributions, those and other significant differences show up. The three barrier distributions are shown in Fig. 4 in the same reduced energy scale of Fig. 3. One sees that the distribution for ^{40}Ca+^{40}Ca (crosses) is the prototype of a single-barrier structure produced by the magic nature of target and projectile, although the position of the barrier (see Ref. [2]) is shifted $\approx$2.5 MeV downwards in energy compared with the standard Akyüz-Winther value. The barrier distribution of ^{40}Ca+^{46}Ti (open dots, see Ref. [6]) has a main peak (whose position is also $\approx$2.5 MeV lower than the Akyüz-Winther value) and a smaller, but clearly visible bump $\simeq$3 MeV higher in energy, due to coupling to the low-lying 2^+ excitation of ^{46}Ti.

The distribution for ^{46}Ti+^{46}Ti (full dots) shows a more complex situation, as commented above, with two peaks of similar strength at approximately 61 MeV and 64 MeV (the Akyüz-Winther barrier is at 64.2 MeV) where the combined effect of the quadrupole excitations in the two nuclei is dominant, possibly including two-phonon excitations. This barrier distribution is similar in nature to the case of ^{58}Ni +^{60}Ni [9] where two-phonon excitations in both target and projectile (four phonons overall) were identified as being responsible for the observed structure with two well resolved peaks of comparable intensity (and a smaller one at low energy, in that case).

Going from ^{40}Ca+^{40}Ca to ^{40}Ca+^{46}Ti and to ^{46}Ti+^{46}Ti one observes a transition where the various relevant couplings do not change the subbarrier fusion yields significantly, and differences can be noticed clearly only when comparing the fusion barrier distributions. A less qualitative interpretation of the evidences for ^{46}Ti+^{46}Ti is mandatory at this point, in view of the hints for effects of complex surface vibrations on subbarrier cross sections.

IV. COUPLED-CHANNELS CALCULATIONS

The coupled-channels (CC) program CCFULL [18] has been employed for the theoretical analysis of the present data on ^{46}Ti+^{46}Ti, in a modified version that allows calculations for fusion of identical nuclei [19]. In CCFULL the number of CC equations is reduced by means of the isocentrifugal ap-

proximation, and an incoming-wave boundary condition is placed inside the barrier. Since simple linear couplings and the adiabatic approximation fail to describe the dynamics of heavy-ion subbarrier fusion [20–22], CCFULL includes the effects of inelastic nonlinear couplings to all orders, and it takes full account of the finite excitation energies of the coupled modes. Vibrational couplings are treated in the harmonic limit. The Akyüz-Winther potential parameters are $V_0=66.07$ MeV, $r_0=1.175$ fm, and $a=0.66$ fm. The corresponding potential barrier has $V_b=64.2$ MeV, $R_b=10.09$ fm, and $\hbar\omega=3.69$ MeV. With respect to this, the bare potential used in the present CC calculations has undergone a few modifications, i.e., the potential well has been chosen to be deeper ($V_0=110$ MeV), but only in order to minimize oscillations in the trasmission coefficients of high partial waves, especially at high energies, so that the ingoing-wave boundary condition is correctly applied.

The radius parameter has been reduced accordingly ($r_0=1.144$ fm), in order to fit the high-energy cross sections; the diffuseness ''*a*'' has not been varied. The resulting barrier ($V_b=63.3$ MeV, $R_b=10.27$ fm, and $\hbar\omega=3.77$ MeV) is slightly (0.9 MeV) lower than the Akyüz-Winther value.

The lowest 2^+ state of ^{46}Ti lies at 0.889 MeV [23]; the deformation parameter for this state was chosen to be $\beta=0.256$ [24], i.e., $\simeq 20\%$ lower than the value derived from the $B(E2)$ strength adopted in Ref. [23]. Using this last value brings to serious overestimations of the subbarrier fusion cross sections even considering one-phonon excitations only. The octupole vibration is at 3.058 MeV [23], with $\beta=0.142$. Q values for all transfer channels are all negative and lower than -2.2 MeV, hence transfer couplings are not expected to be important and have not been considered in the CC calculations.

The results of CCFULL for the cross sections are shown in Fig. 1; the no-coupling limit is also shown for reference. One sees immediately that the effect of the octupole vibration is predicted to be relatively small (short-dashed line), and, since the excitation energy of the 3^- state is large (but not larger than $\hbar\omega=3.77$ MeV), one almost obtains only a ''rigid'' shift of the excitation function towards lower energies (by ≈ 0.6 MeV). Indeed, in Fig. 2 the corresponding barrier distribution (short-dashed line) has a main peak that is shifted with respect to the no-coupling case (dots), and a small second peak appears around 66 MeV.

Structural changes in the barrier distribution are caused by the lower-lying quadrupole excitations, along with larger enhancements of the subbarrier cross sections. Figure 1 shows that the calculation (long-dashed line) considering two-phonon excitations only (i.e., the lowest 2^+ state in *both* colliding nuclei) does not reproduce correctly the low-energy cross sections that are slightly underestimated for $E\leqslant 61$ MeV; the calculated excitation function appears to fall down too sharply with decreasing energy in that range. The corresponding barrier distribution (Fig. 2) has two peaks like the ''experimental'' one but the overall fit is not very good. Better agreement is found, both for cross sections and for barrier distribution, when the calculation includes four quadrupole-phonon states (two in the projectile and two in the target), as shown by the full lines in Figs. 1 and 2. In particular, the shape of the excitation function at low energies is nicely reproduced, and the (more complex) barrier distribution is very near to the experimental evidences. The larger subbarrier cross sections in the four-phonon calculation are generated by the small bump in the barrier distribution visible at $\simeq 59$ MeV.

Overall, the situation is similar to that found for ^{58}Ni $+^{60}$Ni [9], where the target and projectile double-phonon excitations were shown to be essential ingredients of subbarrier fusion yields. The barrier distribution of ^{46}Ti$+^{46}$Ti is ≈ 8 MeV wide, a value very much close to the case of Ni $+$Ni ($\simeq 13$ MeV) when one takes into account the different Z_1Z_2 product. The large and clearly resolved peaks (see again Fig. 2) are characteristic of strong phonon couplings.

However, the two-phonon calculation for ^{58}Ni$+^{60}$Ni manifestly failed even at the qualitative level, while it is still acceptable for the present ^{46}Ti$+^{46}$Ti data. Here it seems that the role of double-phonon excitations in both projectile and target (four phonons) is less essential. The difference between full and long-dashed lines in Fig. 1 is not at all large and its significance is unclear, also in view of the uncertainty in the choice of the deformation parameter for the 2^+ state (see above). This state is anyway more collective than the corresponding one in ^{58,60}Ni, and no loss of collectivity can be claimed for the 4^+ state of ^{46}Ti [23,24], hence we tend to attribute the less important role of double phonons in ^{46}Ti $+^{46}$Ti to the smaller Z_1Z_2 product in this system, which scales down the coupling strengths.

V. SUMMARY AND CONCLUSIONS

Fusion-evaporation cross sections have been measured for the symmetric system ^{46}Ti$+^{46}$Ti near and below the Coulomb barrier. The ''fusion barrier distribution,'' i.e., the second energy derivative of the excitation function, has been extracted from the data. It has a structure with two resolved peaks of comparable intensity, thus indicating couplings to strong surface vibrations.

The comparison of the present data with the corresponding ones for ^{40}Ca$+^{40}$Ca and ^{40}Ca$+^{46}$Ti shows that subbarrier fusion yields are not very different for the three systems in spite of the well-known differences of nuclear structure between ^{40}Ca and ^{46}Ti. On the other hand, more subtle information is hidden in the curvatures of the excitation functions, and shows up clearly in the barrier distributions that are very different in the three cases.

The present data for ^{46}Ti$+^{46}$Ti have been analyzed, within the coupled-channels model, by the code CCFULL that treats the excitation energies of the coupled modes correctly and with full-order couplings. While the octupole vibration is not negligible, the strong quadrupole excitation of ^{46}Ti is dominating. Good agreement is found, both for the cross sections and for the barrier distribution, with the calculation including two quadrupole phonon states in both colliding nuclei, besides the octupole modes, though there is relatively little change with respect to the results obtained with one quadrupole-phonon in each ^{46}Ti. The experimental data and the indications coming from the CC model give a significant degree of similarity between the present system and the previous case of ^{58}Ni$+^{60}$Ni.

ACKNOWLEDGMENTS

We are very grateful to K. Hagino for providing us with the new version of the CCFULL program. We acknowledge the professional work of G. Manente and M. Loriggiola in the preparation of targets of excellent quality. We also thank the XTU Tandem staff for careful and patient work during the experiments.

[1] A.B. Balantekin and N. Takigawa, Rev. Mod. Phys. **70**, 77 (1998).
[2] M. Dasgupta, D.J. Hinde, N. Rowley, and A.M. Stefanini, Annu. Rev. Nucl. Part. Sci. **48**, 401 (1998).
[3] N. Rowley, G.R. Satchler, and P.H. Stelson, Phys. Lett. B **254**, 25 (1991).
[4] J.X. Wei, J.R. Leigh, D.J. Hinde, J.O. Newton, R.C. Lemmon, S. Elfstrom, J.X. Chen, and N. Rowley, Phys. Rev. Lett. **67**, 3368 (1991).
[5] R.C. Lemmon, J.R. Leigh, J.X. Wei, C.R. Morton, D.J. Hinde, J.O. Newton, J.C. Mein, and M. Dasgupta, Phys. Lett. B **316**, 32 (1993).
[6] J.D. Bierman, P. Chan, J.F. Liang, M.P. Kelly, A.A. Sonzogni, and R. Vandenbosch, Phys. Rev. Lett. **76**, 1587 (1996).
[7] C.R. Morton, A.C. Berriman, R.D. Butt, M. Dasgupta, D.J. Hinde, A. Godley, J.O. Newton, and K. Hagino, Phys. Rev. C **64**, 034604 (2001).
[8] C.R. Morton, M. Dasgupta, D.J. Hinde, J.R. Leigh, R.C. Lemmon, J.P. Lestone, J.C. Mein, J.O. Newton, H. Timmers, N. Rowley, and A.T. Kruppa, Phys. Rev. Lett. **72**, 4074 (1994).
[9] A.M. Stefanini, D. Ackermann, L. Corradi, D.R. Napoli, C. Petrache, P. Spolaore, P. Bednarczyk, H.Q. Zhang, S. Beghini, G. Montagnoli, L. Mueller, F. Scarlassara, G.F. Segato, F. Soramel, and N. Rowley, Phys. Rev. Lett. **74**, 864 (1995).
[10] H. Timmers, D. Ackermann, S. Beghini, L. Corradi, J.H. He, G. Montagnoli, F. Scarlassara, A.M. Stefanini, and N. Rowley, Nucl. Phys. **A633**, 421 (1998).
[11] A.M. Stefanini, L. Corradi, A.M. Vinodkumar, Yang Feng, F. Scarlassara, G. Montagnoli, S. Beghini, and M. Bisogno, Phys. Rev. C **62**, 014601 (2000).
[12] H.A. Aljuwair, R.J. Ledoux, M. Beckerman, S.B. Gazes, J. Wiggins, E.R. Cosman, R.R. Betts, S. Saini, and O. Hansen, Phys. Rev. C **30**, 1223 (1984).
[13] A.A. Sonzogni, J.D. Bierman, M.P. Kelly, J.P. Lestone, J.F. Liang, and R. Vandenbosch, Phys. Rev. C **57**, 722 (1998).
[14] S. Beghini, C. Signorini, S. Lunardi, M. Morando, G. Fortuna, A.M. Stefanini, W. Meczynski, and R. Pengo, Nucl. Instrum. Methods Phys. Res. A **239**, 585 (1985).
[15] M. Trotta, A. M. Stefanini, L. Corradi, A. Gadea, F. Scarlassara, S. Beghini, and G. Montagnoli, Phys. Rev. C **65**, 011601(R) (2001).
[16] Ö. Akyüz and A. Winther, in *Nuclear Structure and Heavy-Ion Physics*, Proceedings of the International School of Physics ''Enrico Fermi,'' Course LXXVII, Varenna, edited by R.A. Broglia and R.A. Ricci (North-Holland, Amsterdam, 1981).
[17] H. Esbensen, S.H. Fricke, and S. Landowne, Phys. Rev. C **40**, 2046 (1989).
[18] K. Hagino, N. Rowley, and A.T. Kruppa, Comput. Phys. Commun. **123**, 143 (1999).
[19] K. Hagino (private communication).
[20] H. Esbensen and S. Landowne, Phys. Rev. C **35**, 2090 (1987).
[21] H. Esbensen and B.B. Back, Phys. Rev. C **54**, 3109 (1996).
[22] K. Hagino, N. Takigawa, M. Dasgupta, D.J. Hinde, and J.R. Leigh, Phys. Rev. C **55**, 276 (1997).
[23] S.-C. Wu, Nucl. Data Sheets **91**, 1 (2000).
[24] M. Fujiwara, S. Morinobu, M. Tosaki, H. Ito, I. Katayama, H. Ikegami, S.I. Hayakawa, N. Ikeda, H. Ohsumi, A. Higashi, and K. Katori, Phys. Rev. C **35**, 1257 (1987).